Running head

PHYLODYNAMIC MODEL ADEQUACY

Title

Phylodynamic model adequacy using posterior predictive simulations

Authors

Sebastian Duchene[1]*, Remco Bouckaert[2,3], David A. Duchene[4], Tanja Stadler[5,6], Alexei J. Drummond[2]

[1]Department of Biochemistry and Molecular Biology, Bio21 Molecular Science and Biotechnology Institute, University of Melbourne, Australia.

[2]Centre for Computational Evolution, University of Auckland, Auckland, New Zealand.

[3]Max Planck Institute for the Science of Human History, Jena, Germany.

[4]School of Life and Environmental Sciences, University of Sydney, Sydney, Australia.

[5]Department of Biosystems Science and Engineering, ETH Zurich, Basel, Switzerland.

[6]Swiss Institute of Bioinformatics, Lausanne, Switzerland.

* To whom correspondence should be addressed:

Sebastian Duchene

Email: sebastian.duchene@unimelb.edu.au

Abstract

Rapidly evolving pathogens, such as viruses and bacteria, accumulate genetic change at a similar timescale over which their epidemiological processes occur, such that it is possible to make inferences about their infectious spread using phylogenetic time-trees. For this purpose it is necessary to choose a phylodynamic model. However, the resulting inferences are contingent on whether the model adequately describes key features of the data. Model adequacy methods allow formal rejection of a model if it cannot generate the main features of the data. We present TreeModelAdequacy (TMA), a package for the popular BEAST2 software, that allows assessing the adequacy of phylodynamic models. We illustrate its utility by analysing phylogenetic trees from two viral outbreaks of Ebola and H1N1 influenza. The main features of the Ebola data were adequately described by the coalescent exponential-growth model, whereas the H1N1 influenza data was best described by the birth-death SIR model.

Keywords

Model adequacy, Bayesian phylogenetics, Phylodynamics, Viral evolution, Posterior predictive simulation, BEAST2

Phylogenetic trees depict the evolutionary relationships between groups of organisms. In the context of infectious diseases, pathogen genetic data can be used to infer such trees. By

assuming a substitution model and including independent information about time, one can calibrate the molecular clock to obtain time-trees, where the branch lengths correspond to units of time, and internal nodes of the tree represent the timing of divergence events. For rapidly evolving viruses and bacteria it is possible to use the sampling times as time-calibrations (Drummond et al. 2003; Rieux and Balloux 2016). In these organisms, genetic change and epidemiological or ecological processes occur over a similar timescale. Thus, time-trees can be informative about epidemiological dynamics, a field of research known as phylodynamics (Holmes et al. 1993; Grenfell et al. 2004; Kühnert et al. 2011; Volz et al. 2013).

Phylodynamic models describe the distribution of node times, branch lengths, and sampling times. In full Bayesian phylogenetic analyses, the tree, parameters for the molecular clock, the substitution model and the phylodynamic model can be estimated simultaneously using molecular data. In this Bayesian framework, the phylodynamic model is effectively a 'tree prior' (e.g. du Plessis and Stadler 2015). The simplest phylodynamic models are the coalescent exponential-growth (CE) and the coalescent constant-size (CC). These two models have very different expectations about the shape of phylogenetic trees, with exponentially growing populations tending to produce trees with longer external branches than those evolving under constant population sizes (O'Meara, 2012; Volz et al., 2013). Alternative phylodynamic models are the birth-death models, which include a parameter to describe the sampling rate, so they have an expectation on the number of taxa and their distribution over time (Stadler 2010; Stadler et al. 2012).

Choosing an appropriate model is important to draw reliable inferences from parameters of interest. For instance, the CE and the constant birth-death (BD) models can estimate the basic reproductive number, R_0 (Frost & Volz, 2010; Stadler et al., 2012; Volz et al., 2013),

which is defined as the average number of new cases that a single case will generate over the course of its infection in a fully susceptible population (Anderson and May 1979, 1992). Failing to account for complex epidemiological dynamics can bias the estimate of this key parameter (Stadler et al. 2014; Alkhamis et al. 2016; Ratmann et al. 2016). A Bayesian approach to selecting a phylodynamic model is to estimate marginal likelihoods for a pool of models and selecting that with the highest marginal likelihood (Baele et al. 2012; Baele et al. 2016), but it is also possible to obtain weighted averages of parameter estimates based on the support for each model (e.g. Baele, Li, Drummond, Suchard, & Lemey, 2013; R. Bouckaert & Drummond, 2017; Huelsenbeck, Larget, & Alfaro, 2004; Li & Drummond, 2012).

Model adequacy in phylogenetics

Model selection methods only allow a relative comparison of a set of models, but they cannot determine whether any of the models in question could have generated key features of the data at hand (i.e. absolute model fit). Such information however is key to avoid unreliable inferences from a model and to improve our understanding of the biological processes that produced the data. Absolute model fit can be assessed via model adequacy methods, where a model is considered 'adequate' if it is capable of generating the main features of the empirical data. Consequently, model adequacy allows the user to formally reject a model or to identify aspects of the data that are poorly described, instead of ranking it with respect to other models, as is the case with model testing (e.g. Goldman 1993; Bollback 2002; Ripplinger and Sullivan 2010; Brown 2014).

Model adequacy is typically conducted by fitting a model to the empirical data, and generating synthetic data from the model in question, a procedure that is similar to a parametric bootstrap (Goldman 1993). The adequacy of the model is determined depending

on whether the synthetic data are similar to the empirical data, according to a descriptive test statistic (Gelman and Shalizi 2013; Gelman et al. 2014). The test statistics should summarise key aspects of the data or a combination of the data and parameter estimates (Gelman et al. 1996). Examples of test statistics that have been used to assess the substitution model include the multinomial likelihood or a measure of compositional homogeneity (Goldman 1993; Huelsenbeck et al. 2001; Foster 2004). The joint clock model and tree prior key can be assessed using the expected number of substitutions in individual branch lengths of the tree as test statistics (Duchêne et al. 2015). For DNA barcoding the number of OTUs and multinomial likelihood have been shown to be effective test statistics (Barley and Thomson 2016). Phylodynamic and diversification models are fitted to phylogenetic trees and their parameters depend on the distribution of nodes, such that some useful test statistics include the ratio of external to internal branch lengths, the tree height, and measures of phylogenetic tree imbalance (Revell et al. 2005, 2008; Drummond and Suchard 2008; Höhna et al. 2015). Clearly, designing test statistics is not trivial, but they should attempt to explicitly test some of the assumptions of the model. For example, the CE and CC models have different expectations of the ratio of external to internal branch lengths, such that this may be a useful test statistic.

Bayesian model adequacy

Bayesian model adequacy consists of a posterior predictive framework (Rubin 1981, 1984; Bollback 2002; Brown 2014a, 2014b; Lewis et al. 2014; Höhna et al. 2017). The posterior distribution of the model in question is approximated given the empirical data, for example using Markov chain Monte Carlo (MCMC). Samples from the MCMC are drawn to simulate data sets under the model used for the empirical analysis. For example, the posterior distribution of the growth rate and population size parameters of the CE model can be sampled to simulate phylogenetic trees. Such simulations are known as posterior predictive

simulations. Test statistics are then calculated for every posterior predictive simulation (i.e. for every simulated tree) to generate a distribution of values according to the model. A posterior predictive probability, similar to the frequentist *p*-value, can be calculated by determining where the value of the test statistic for the empirical data (i.e. the empirical phylogenetic tree) falls with respect to the posterior predictive distribution (Gelman et al. 2014). Following Gelman et al. (2014) we refer to the posterior predictive probability as p_B to differentiate it from the frequentist *p*-value. A useful guideline to determine whether the model is adequate is to determine whether a test statistic within the 95% credible interval (Bollback 2002; Brown 2014a). This approach is sometimes conservative, particularly when test statistics do not follow a Gaussian distribution, and other methods of calculating posterior predictive probabilities are also possible (Gelman et al. 2014; Höhna et al. 2017). Combining multiple test statistics leads to multiple testing, which can be addressed by using a multivariate p_B values (Drummond and Suchard 2008). However, Gelman et al. (2014) suggest considering each test statistically separately to assess individual aspects of the model and the data, which is the approach taken here.

Bayesian model adequacy is similar to Approximate Bayesian Computation (ABC) techniques in that both methods use test statistics from simulated data. The aim of ABC is to approximate the posterior by comparing test statistics from simulations from the prior and the empirical data (Csilléry et al. 2010; Ratmann et al. 2012; Poon 2015), which sometimes leads to biases for model testing (Robert et al. 2011). In contrast, in model adequacy the simulations are generated from the posterior distribution and they are not used to approximate the posterior. In spite of these differences, test statistics developed for ABC can be useful to assess model adequacy.

"TreeModelAdequacy" package in BEAST2

158 We implemented a computational framework to assess the adequacy of phylodynamic
159 models as a package for BEAST2 (Bouckaert et al., 2014). Analyses as outlined in Fig 1 are
160 easy to set up through BEAUti, the graphical user interface for BEAST, to generate an xml
161 file with the tree, the model, and test statistics. Our package, TreeModelAdequacy (TMA),
162 takes a tree with branch lengths proportional to time. The tree can be a summary tree from
163 BEAST2, or estimated using a different method.
164
165 We fit phylodynamic models available in BEAST2 by approximating the posterior
166 distribution of the parameters of the model using MCMC. To generate the posterior
167 predictive simulations, we draw random samples from the posterior for the parameters
168 from the MCMC after removing the burn-in phase, and we simulate phylogenetic trees
169 using stochastic simulations and master equations using MASTER (Vaughan and
170 Drummond 2013) or the coalescent simulator in BEAST2. The last step consists in
171 calculating test statistics for the empirical data and for the posterior predictive simulations,
172 which depends on the TreeStat2 package (available at
173 http://github.com/alexeid/TreeStat2). The user can select a large number of test statistics
174 (Supplementary material). At the end of the analysis, p_B values and quantiles for the
175 posterior predictive distribution are shown, but they can also be visualised in Tracer
176 (available at: http://beast.bio.ed.ac.uk/tracer) or using an R script included in the package.
177 At present, the range of phylodynamic models that can be assessed includes the CC and CE
178 coalescent models, the constant BD with serial sampling (Stadler et al. 2012), and the birth-
179 death susceptible-infected-recovered model (BDSIR; Kühnert et al. 2014).
180
181 Our implementation allows parallelisation of the tree simulation step, which can increase
182 computational speed when the simulation conditions require extensive calculations. This
183 step can also be conducted independently on a computer cluster. Our standalone

184 application TreeModelAdequacyAnalyser can also compute test statistics and p_B values,
185 even for trees generated in a different program than BEAST2, given that the posterior
186 predictive trees are provided. TMA is open source and freely available under a LGPL licence.
187 It can be downloaded from BEAUTi2 (part of BEAST2), and the documentation and
188 example files are available at: http://github.com/sebastianduchene/tree_model_adequacy.
189
190 To verify our implementation, we conducted a simple simulation experiment. We simulated
191 100 trees under each of the four phylodynamic models (CC, CE, BD, and BDSIR) using
192 BEAST2 and MASTER and analysed them with the matching model. We assessed their
193 adequacy according to nine test statistics (Supplementary material). The parameters for our
194 simulations were based on analyses of 72 whole genome sequences of Ebola virus (Gire et
195 al. 2014). We found that the p_B values for all test statistics were between 0.025 and 0.975 for
196 about 95% of each set of simulations, indicating that our implementation is correct
197 (Supplementary material).
198
199 **Phylodynamic model adequacy in empirical virus data**
200 *West African Ebola virus*
201 We obtained a phylogenetic tree inferred in a previous study from 72 Ebola virus whole
202 genome samples collected during the 2013-2016 epidemic (Gire et al. 2014). The samples
203 were collected from May to July 2014 in Sierra Leone. These data have been used in
204 previous studies to estimate epidemiological parameters, with estimates of R_o ranging from
205 1.5 to 2.5, depending on the phylodynamic model (Stadler et al., 2014; Volz & Pond, 2014).
206 An important consideration about our analysis is that we assume that the tree topology and
207 divergence time estimates are sufficiently accurate and that the data are informative.
208

We inferred phylodynamic parameters for the Ebola virus tree using four models; CC, CE, the BD, and the BDSIR (Kühnert et al. 2014). The CE, BD, and BDSIR models can estimate R_o if information about the sampling process (for the birth-death models) or present number of infected individuals (for the coalescent) is available. In this case, we assumed that the sampling proportion was 0.7 (Gire et al. 2014) by fixing this parameter in the BD and BDSIR models. For the remaining parameters of these two models, we used the same prior distributions as in a previous analysis of these data (Stadler et al. 2014). For the CE model we used a Laplace distribution and a $1/x$ distribution as priors for the growth rate and for the effective population size, respectively. We ran an MCMC of 10^7 steps and generated 1,000 posterior predictive simulations, and we computed four test statistics.

To compare the different models, we calculated p_B for four test statistics; the tree height, the slope ratio of a lineages-through-time (LTT) plot, the ratio of external to internal branch lengths, and the Colless index of phylogenetic imbalance (Fig. 2; Supplementary material). Importantly, the slope ratio of the LTT plot has been found to be informative for inferring epidemiological parameters using ABC (Saulnier et al. 2017).

In the CC model the p_B was < 0.05 for all test statistics, with the exception of the tree height at 0.06 (Fig. 2 and Supplementary material Fig. S1). The CE and BD models described these data better, with most p_B values between 0.11 and 0.56. The p_p value for the Colless index in the CE model was the lowest for both of these models, at 0.04. The BDSIR model had overall low p_B values, from to 0.01 to 0.18, with the lowest values found for the ratio of external to internal branch lengths (0.03) and for the slope ratio of the LTT plot (0.01). The fact that most p_B values for the CE and BD models frequently fall near the centre of the posterior predictive distributions is consistent with the rapid spread that Ebola virus was undergoing at the time the sequences were collected.

For the CE, BD, and BDISIR models we can estimate R_o and the infectious period, $1/\delta$. The R_o median estimates were: 1.6 (95% credible interval (CI): 1.12 – 2.2) for the BD, 1.21 (95% CI: 1.1 – 1.5), for the CE, and 1.59 (95% CI: 1.22 – 1.94) for the BDSIR. Estimates for the infectious period in calendar days were: 5.46 (95% CI: 4.14 – 7.24) for the BD, 2.90 (95% CI: 1.75 – 5.50) for the CE, and 5.21 (95% CI: 4.24 – 7.02) for the BDSIR. The estimates from these models were very similar and overlapped with those from previous studies (Stadler et al. 2014). Although the BDSIR did not capture some of the main features of these data, this model is similar to the BD when the number of susceptible individuals is very large, which probably explains the overlap in R_o estimates between these models.

2009 H1N1 Influenza

We obtained a phylogenetic tree from a previous study (Hedge et al. 2013),which was estimated from 328 whole genome samples from the 2009 H1N1 Influenza pandemic. The samples were collected from April to December 2009, such that they encompass a large portion of the duration of the pandemic. We used a similar method as for the Ebola virus phylogenetic tree to fit the four phylodynamic models (CC, CE, BD, and BDSIR). However, instead of fixing the sampling proportion we used an informative prior distribution of the infectious period via the *becomeUnifectiousRate* parameter, with a normal distribution of mean 85 and standard deviation of 15 (corresponding to an infectious period of about 4.45 days).

The CC and CE models had p_B values of 0.00 for all four test statistics, such that they did not adequately describe any of these aspects of the tree. The BD model had p_B values of 0.53 and 0.09 for the tree height and the slope ratio of the LTT plot, and of 0.00 for the ratio of external to internal branch lengths (Fig. 2 and Supplementary material Fig. S2). In contrast,

261 the BDSIR model overall described the H1N1 tree better overall than the other three
262 models, with p_B values of between 0.07 and 0.44. This result is consistent with the sampling
263 time of the data, which includes the start of the pandemic and the decline in the number of
264 infections towards the end of the year. We calculated an R_o of mean 3.01 (95% CI: 2.5 – 3.7)
265 at the start of the pandemic in January that declined to $R_o < 1$ around June, when infectious
266 spread was lower. This estimate is similar to those made in previous studies based on
267 census data (Forsberg White et al. 2009), but in the higher range of those based on the CE
268 model for samples collected in early stages of the pandemic (e.g. Hedge et al. 2013). For
269 comparison, the R_o estimate from the BD model, which appeared inadequate, was
270 substantially lower, with a mean of 1.02 (95% CI: 1.00 – 1.03).
271
272 **Conclusion**
273 Model adequacy methods are useful to understand the biological processes that generate
274 the data, such as the evolutionary branching process. For example, our approach reveals
275 that in July of 2014 the West African Ebola outbreak was still growing exponentially and
276 that the 2009 H1N1 influenza virus pandemic had evidence of a depletion of susceptible
277 individuals in December. In some cases, identifying models that indadequately describe key
278 aspects of the data may improve estimates of parameters of interest, such as R_o in our H1N1
279 influenza analyses. One consideration of our approach is that it requires an accurate
280 estimate of a single phylogenetic tree. Clearly, the phylogenetic tree should be inferred
281 using informative sequence data and the sensitivity to the prior should be carefully
282 examined (Ritchie et al. 2016; Boskova et al. 2018; Möller et al. 2018), which is also the case
283 for any Bayesian analysis. For example, a tree estimated from uninformative sequence data
284 will be driven by the prior and will necessarily appear to be adequately described by the
285 matching model, potentially leading to increased rates of type 2 errors. A limitation of our
286 method is that it does not account for phylogenetic uncertainty, which can be addressed by

comparing sets of trees from the posterior with those from the posterior predictive distribution. However, this approach will require the development of new test statistics and model assessment criteria. Model adequacy in phylogenetics will benefit from further development of methods to assess more sophisticated phylodynamic models, such as those that account for population structure (Kühnert et al. 2016; Müller et al. 2017a, 2017b; Volz and Siveroni 2018), and techniques to improve the interpretation of p_B values for test statistics that are not normally distributed, such at the Colless index. Model adequacy software, such as TMA, will be key to address these questions.

Acknowledgements

The authors thank Timothy Vaughan for valuable discussions. SD was supported by a McKenzie fellowship and a Dyason grant from the University of Melbourne. AJD was supported by a Rutherford fellowship (http://www.royalsociety.org.nz/programmes/funds/rutherford-discovery/) from the Royal Society of New Zealand. TS was supported in part by the European Research Council under the Seventh Framework Programme of the European Commission (PhyPD: grant agreement number 335529).

Conflict of interest

The authors gave final approval to the manuscript and have no conflict of interest to declare.

Author contributions

SD, RB, and AJD wrote the computer code. SD analysed the data. TS, SD, and AJD designed the experiments. SD wrote the manuscript with input from all the authors.

Figure Legends

Fig 1. Posterior predictive simulation framework implemented in the TreeModelAdequacy package. Step (1) consists in Bayesian analysis in BEAST under model M to estimate the posterior distribution of parameters η, shown with the arrow and posterior density in orange. In step (2) samples from the posterior are drawn to simulate phylogenetic trees, known as posterior predictive simulations, using MASTER as shown by the green arrow. In step (3) the posterior predictive simulations are analysed in TreeStat to generate the posterior predictive distribution of test statistic T_α, shown by the blue arrow and probability density. Finally, T_α is also computed for the tree from the empirical data using TreeStat, shown by the red arrow, to calculate a posterior predictive probability (p_B). Test statistics and p_B values can also be computed for trees generated in other programs using TreeModelAdequacyAnalyser, given that the tree from the empirical data and the posterior predictive simulations are provided.

Fig 2. Model adequacy results for the two empirical data sets, West African Ebola and 2009 H1N1 influenza. The histograms show the distribution of two test statistics, the tree height and the slope ratio of the lineages-through-time (LTT) plot, for the posterior predictive simulations. The black points also show the distribution of the test statistics, and they have been jittered along the *y*-axis to improve visualisation. The red lines denote the value for the tree estimated from the empirical data. The posterior predictive *p*-value, p_B, is shown for each test statistic. A feature of the empirical phylogenetic tree described by a test statistic, such as the tree height, is considered adequately described by the model if the empirical value falls within the 95% quantile range of the posterior predictive distribution, such that the $p_B > 0.05$. Two more test statistics were computed, the ratio of external to internal branch lengths and the Colless index, which are shown in Supplementary material Fig. S1. Note that for the H1N1 influenza analyses, the values are shown in a $\log_{10}$ scale.

Supplementary figure captions

Fig S1. Model adequacy results for Ebola virus data with four test statistics. The colours and symbols match those in Fig 2.

Fig S2. Model adequacy results for H1N1 influenza data with four test statistics. The colours and symbols match those in Fig 2. Note that the values are shown in $\log_{10}$ scale.

351 **References**

352 Alkhamis M.A., Perez A.M., Murtaugh M.P., Wang X., Morrison R.B. 2016. Applications of
353 Bayesian phylodynamic methods in a recent US porcine reproductive and respiratory
354 syndrome virus outbreak. Front. Microbiol. 7:67.
355 Anderson R.M., May R.M. 1979. Population biology of infectious diseases: Part I. Nature.
356 280:361.
357 Anderson R.M., May R.M. 1992. Infectious diseases of humans: dynamics and control.
358 Oxford university press.
359 Baele G., Lemey P., Bedford T., Rambaut A., Suchard M.A., Alekseyenko A. V. 2012.
360 Improving the accuracy of demographic and molecular clock model comparison while
361 accommodating phylogenetic uncertainty. Mol. Biol. Evol. 29:2157–2167.
362 Baele G., Lemey P., Suchard M.A. 2016. Genealogical working distributions for Bayesian
363 model testing with phylogenetic uncertainty. Syst. Biol. 65:250–264.
364 Baele G., Li W.L.S., Drummond A.J., Suchard M.A., Lemey P. 2013. Accurate model
365 selection of relaxed molecular clocks in bayesian phylogenetics. Mol. Biol. Evol.
366 30:239–243.
367 Barley A.J., Thomson R.C. 2016. Assessing the performance of DNA barcoding using
368 posterior predictive simulations. Mol. Ecol. 25:1944–1957.
369 Bollback J.P. 2002. Bayesian model adequacy and choice in phylogenetics. Mol. Biol. Evol.
370 19:1171–1180.
371 Boskova V., Stadler T., Magnus C. 2018. The influence of phylodynamic model
372 specifications on parameter estimates of the Zika virus epidemic. Virus Evol. 4:vex044.
373 Bouckaert R., Drummond A.J. 2017. bModelTest: Bayesian phylogenetic site model
374 averaging and model comparison. BMC Evol. Biol. 17:42.
375 Bouckaert R., Heled J., Kühnert D., Vaughan T., Wu C.-H., Xie D., Suchard M.A., Rambaut
376 A., Drummond A.J. 2014. BEAST 2: a software platform for Bayesian evolutionary
377 analysis. PLOS Comput. Biol. 10:e1003537.
378 Brown J.M. 2014a. Detection of implausible phylogenetic inferences using posterior
379 predictive assessment of model fit. Syst. Biol. 63:334–348.
380 Brown J.M. 2014b. Predictive approaches to assessing the fit of evolutionary models. Syst.
381 Biol. 63:289–292.
382 Csilléry K., Blum M.G.B., Gaggiotti O.E., François O. 2010. Approximate Bayesian
383 computation (ABC) in practice. Trends Ecol. Evol. 25:410–418.
384 Drummond A.J., Pybus O.G., Rambaut A., Forsberg R., Rodrigo A.G. 2003. Measurably

evolving populations. Trends Ecol. Evol. 18:481–488.

Drummond A.J., Suchard M.A. 2008. Fully Bayesian tests of neutrality using genealogical summary statistics. BMC Genet. 9:68.

Duchêne D.A., Duchêne S., Holmes E.C., Ho S.Y.W. 2015. Evaluating the adequacy of molecular clock models using posterior predictive simulations. Mol. Biol. Evol. 32:2896–2995.

Forsberg White L., Wallinga J., Finelli L., Reed C., Riley S., Lipsitch M., Pagano M. 2009. Estimation of the reproductive number and the serial interval in early phase of the 2009 influenza A/H1N1 pandemic in the USA. Influenza Other Respi. Viruses. 3:267–276.

Foster P.G. 2004. Modeling compositional heterogeneity. Syst. Biol. 53:485–495.

Frost S.D.W., Volz E.M. 2010. Viral phylodynamics and the search for an "effective number of infections." Philos. Trans. R. Soc. London B Biol. Sci. 365:1879–1890.

Gelman A., Carlin J.B., Stern H.S., Dunson D.B., Vehtari A., Rubin D.B. 2014. Model checking. Bayesian data analysis. Boca Raton, Florida: CRC press Boca Raton, FL. p. 141–163.

Gelman A., Meng X.-L., Stern H. 1996. Posterior predictive assessment of model fitness via realized discrepancies. Stat. Sin.:733–760.

Gelman A., Shalizi C.R. 2013. Philosophy and the practice of Bayesian statistics. Br. J. Math. Stat. Psychol. 66:8–38.

Gire S.K., Goba A., Andersen K.G., Sealfon R.S.G., Park D.J., Kanneh L., Jalloh S., Momoh M., Fullah M., Dudas G. 2014. Genomic surveillance elucidates Ebola virus origin and transmission during the 2014 outbreak. Science (80-.). 345:1369–1372.

Goldman N. 1993. Simple diagnostic statistical tests of models for DNA substitution. J. Mol. Evol. 37:650–661.

Grenfell B.T., Pybus O.G., Gog J.R., Wood J.L.N., Daly J.M., Mumford J.A., Holmes E.C. 2004. Unifying the epidemiological and evolutionary dynamics of pathogens. Science. 303:327–332.

Hedge J., Lycett S.J., Rambaut A. 2013. Real-time characterization of the molecular epidemiology of an influenza pandemic. Biol. Lett. 9:20130331.

Höhna S., Coghill L.M., Mount G.G., Thomson R.C., Brown J.M. 2017. P3: Phylogenetic Posterior Prediction in RevBayes. Mol. Biol. Evol.

Höhna S., May M.R., Moore B.R. 2015. TESS: an R package for efficiently simulating phylogenetic trees and performing Bayesian inference of lineage diversification rates.

419 Bioinformatics. 32:789–791.
420 Holmes E.C., Zhang L.Q., Simmonds P., Rogers A.S., Brown A.J.L. 1993. Molecular
421 investigation of human immunodeficiency virus (HIV) infection in a patient of an HIV-
422 infected surgeon. J. Infect. Dis. 167:1411–1414.
423 Huelsenbeck J.P., Larget B., Alfaro M.E. 2004. Bayesian phylogenetic model selection using
424 reversible jump Markov chain Monte Carlo. Mol. Biol. Evol. 21:1123–1133.
425 Huelsenbeck J.P., Ronquist F., Nielsen R., Bollback J.P. 2001. Bayesian inference of
426 phylogeny and its impact on evolutionary biology. Science (80-.). 294:2310–2314.
427 Kühnert D., Stadler T., Vaughan T.G., Drummond A.J. 2014. Simultaneous reconstruction of
428 evolutionary history and epidemiological dynamics from viral sequences with the
429 birth–death SIR model. J. R. Soc. Interface. 11:20131106.
430 Kühnert D., Stadler T., Vaughan T.G., Drummond A.J. 2016. Phylodynamics with migration:
431 A computational framework to quantify population structure from genomic data. Mol.
432 Biol. Evol. 33:2102–2116.
433 Kühnert D., Wu C.H., Drummond A.J. 2011. Phylogenetic and epidemic modeling of rapidly
434 evolving infectious diseases. Infect. Genet. Evol. 11:1825–1841.
435 Lewis P.O., Xie W., Chen M.-H., Fan Y., Kuo L. 2014. Posterior predictive Bayesian
436 phylogenetic model selection. Syst. Biol. 63:309–321.
437 Li W.L.S., Drummond A.J. 2012. Model averaging and Bayes factor calculation of relaxed
438 molecular clocks in Bayesian phylogenetics. Mol. Biol. Evol. 29:751–761.
439 Möller S., du Plessis L., Stadler T. 2018. Impact of the tree prior on estimating clock rates
440 during epidemic outbreaks. Proc. Natl. Acad. Sci. USA. 115:4200–4205.
441 Müller N.F., Rasmussen D.A., Stadler T. 2017a. MASCOT: Parameter and state inference
442 under the marginal structured coalescent approximation. bioRxiv.:188516.
443 Müller N.F., Rasmussen D.A., Stadler T. 2017b. The Structured Coalescent and Its
444 Approximations. Mol. Biol. Evol. 34:2970–2981.
445 O'Meara B.C. 2012. Evolutionary inferences from phylogenies: a review of methods. Annu.
446 Rev. Ecol. Evol. Syst. 43:267–285.
447 du Plessis L., Stadler T. 2015. Getting to the root of epidemic spread with phylodynamic
448 analysis of genomic data. Trends Microbiol. 23:383–386.
449 Poon A.F.Y. 2015. Phylodynamic inference with kernel ABC and its application to HIV
450 epidemiology. Mol. Biol. Evol. 32:2483–2495.
451 Ratmann O., Donker G., Meijer A., Fraser C., Koelle K. 2012. Phylodynamic inference and
452 model assessment with approximate bayesian computation: influenza as a case study.

PLoS Comput. Biol. 8:e1002835.
Ratmann O., Hodcroft E.B., Pickles M., Cori A., Hall M., Lycett S., Colijn C., Dearlove B., Didelot X., Frost S. 2016. Phylogenetic Tools for Generalized HIV-1 Epidemics: Findings from the PANGEA-HIV Methods Comparison. Mol. Biol. Evol. 34:185–203.
Revell L.J., Harmon L.J., Collar D.C. 2008. Phylogenetic signal, evolutionary process, and rate. Syst. Biol. 57:591–601.
Revell L.J., Harmon L.J., Glor R.E. 2005. Under-parameterized model of sequence evolution leads to bias in the estimation of diversification rates from molecular phylogenies. Syst. Biol. 54:973–983.
Rieux A., Balloux F. 2016. Inferences from tip-calibrated phylogenies: a review and a practical guide. Mol. Ecol. 25:1911–1924.
Ripplinger J., Sullivan J. 2010. Assessment of substitution model adequacy using frequentist and Bayesian methods. Mol. Biol. Evol. 27:2790–2803.
Ritchie A.M., Lo N., Ho S.Y.W. 2016. The impact of the tree prior on molecular dating of data sets containing a mixture of inter-and intraspecies sampling. Syst. Biol. 66:413–425.
Robert C.P., Cornuet J.-M., Marin J.-M., Pillai N.S. 2011. Lack of confidence in approximate Bayesian computation model choice. Proc. Natl. Acad. Sci. USA. 108:15112–15117.
Rubin D.B. 1981. Estimation in parallel randomized experiments. J. Educ. Stat. 6:377–401.
Rubin D.B. 1984. Bayesianly justifiable and relevant frequency calculations for the applied statistician. Ann. Stat. 12:1151–1172.
Saulnier E., Alizon S., Gascuel O. 2017. Assessing the accuracy of Approximate Bayesian Computation approaches to infer epidemiological parameters from phylogenies. PLOS Comput. Biol. 13:e1005416.
Stadler T. 2010. Sampling-through-time in birth-death trees. J. Theor. Biol. 167:696–404.
Stadler T., Kouyos R., von Wyl V., Yerly S., Böni J., Bürgisser P., Klimkait T., Joos B., Rieder P., Xie D. 2012. Estimating the basic reproductive number from viral sequence data. Mol. Biol. Evol. 29:347–357.
Stadler T., Kühnert D., Rasmussen D.A., du Plessis L. 2014. Insights into the early epidemic spread of Ebola in Sierra Leone provided by viral sequence data. PLoS Curr. 6.
Vaughan T.G., Drummond A.J. 2013. A stochastic simulator of birth–death master equations with application to phylodynamics. Mol. Biol. Evol. 30:1480–1493.
Volz E., Pond S. 2014. Phylodynamic analysis of Ebola virus in the 2014 Sierra Leone epidemic. PLoS Curr. 6.

Volz E., Siveroni I. 2018. Bayesian phylodynamic inference with complex models. bioRxiv.:268052.

Volz E.M., Koelle K., Bedford T. 2013. Viral phylodynamics. PLOS Comput. Biol. 9:e1002947.

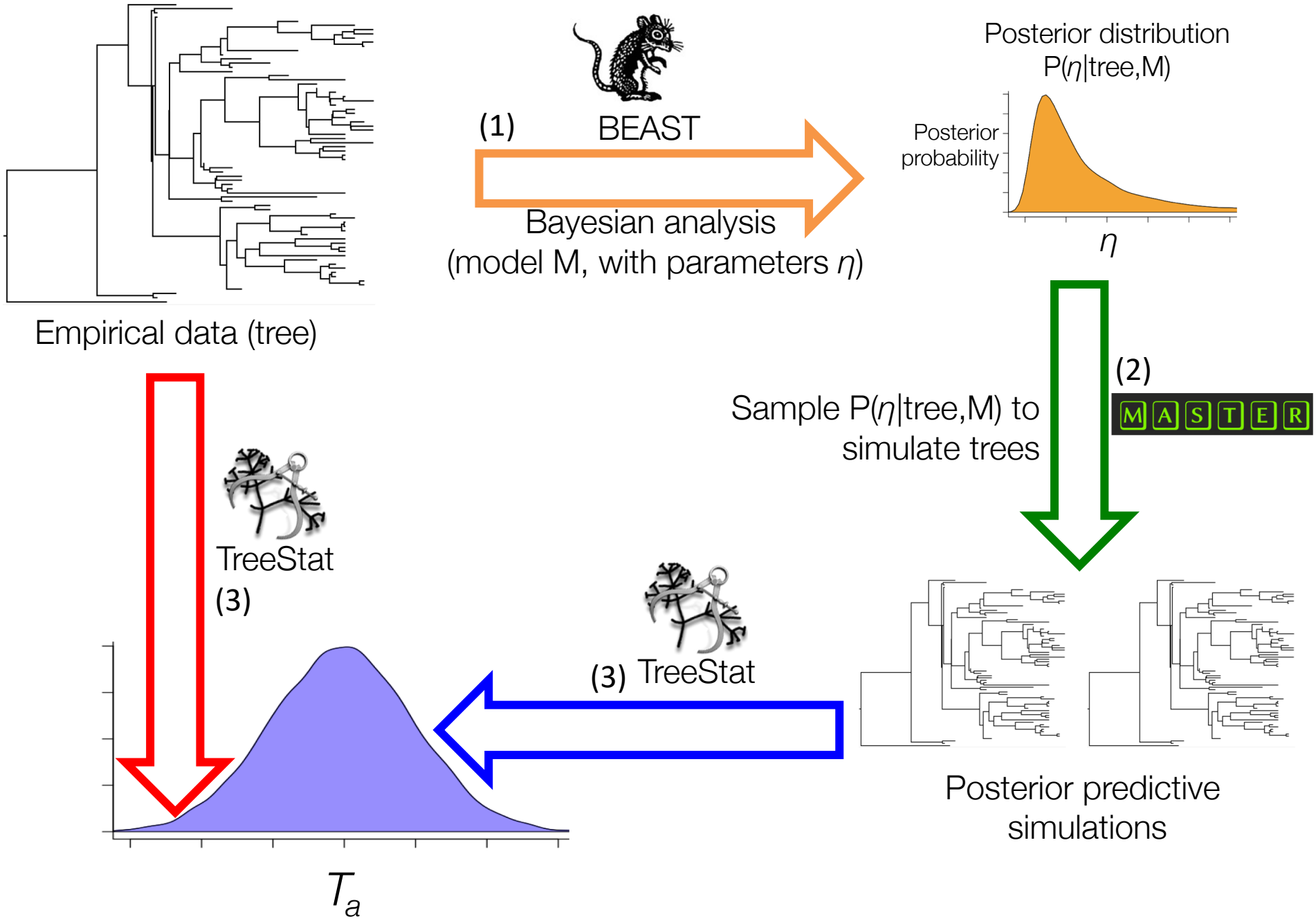
Empirical data (tree)
(1)
BEAST
Bayesian analysis
(model M, with parameters η)
Posterior distribution
P(η|tree,M)
Posterior
probability
η
(2)
MASTER
Sample P(η|tree,M) to
simulate trees
Posterior predictive
simulations
(3) TreeStat
TreeStat
(3)
T_a

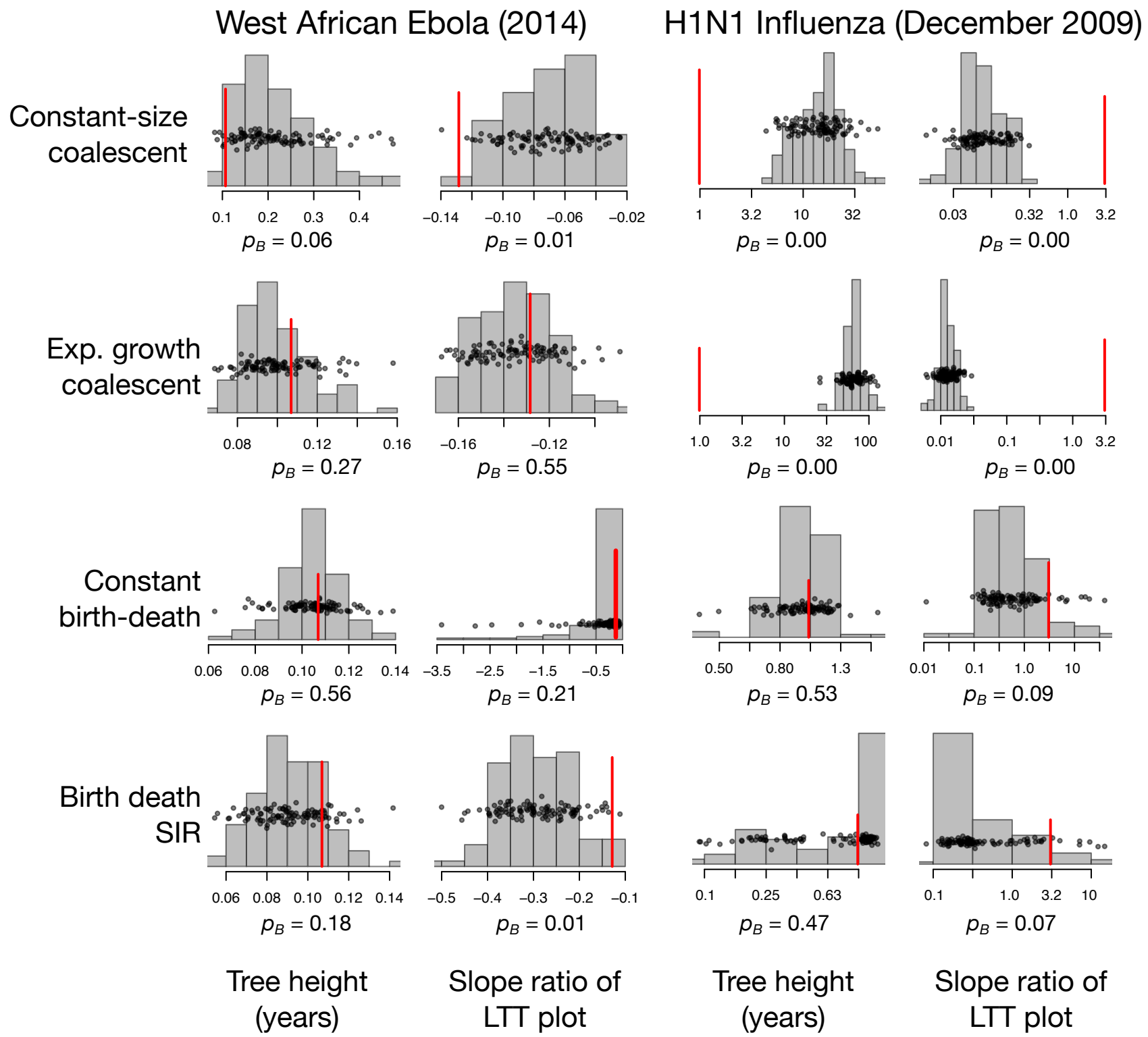
West African Ebola (2014)
H1N1 Influenza (December 2009)
Constant-size coalescent
Exp. growth coalescent
Constant birth-death
Birth death SIR
0.1 0.2 0.3 0.4
p_B = 0.06
−0.14 −0.10 −0.06 −0.02
p_B = 0.01
1 3.2 10 32
p_B = 0.00
0.03 0.32 1.0 3.2
p_B = 0.00
0.08 0.12 0.16
p_B = 0.27
−0.16 −0.12
p_B = 0.55
1.0 3.2 10 32 100
p_B = 0.00
0.01 0.1 1.0 3.2
p_B = 0.00
0.06 0.08 0.10 0.12 0.14
p_B = 0.56
−3.5 −2.5 −1.5 −0.5
p_B = 0.21
0.50 0.80 1.3
p_B = 0.53
0.01 0.1 1.0 10
p_B = 0.09
0.06 0.08 0.10 0.12 0.14
p_B = 0.18
−0.5 −0.4 −0.3 −0.2 −0.1
p_B = 0.01
0.1 0.25 0.63
p_B = 0.47
0.1 1.0 3.2 10
p_B = 0.07
Tree height (years)
Slope ratio of LTT plot
Tree height (years)
Slope ratio of LTT plot